JOURNAL OF CATALYSIS 157, 301–311 (1995)

Chromia Supported on Titania

V. Preparation and Characterization of Supported CrO_2, CrOOH, and Cr_2O_3

K. Köhler,[1] M. Maciejewski, H. Schneider, and A. Baiker[2]

Department of Chemical Engineering and Industrial Chemistry, Swiss Federal Institute of Technology, ETH-Zentrum, CH-8092 Zürich, Switzerland

Received March 1, 1995; revised May 1, 1995; accepted July 25, 1995

Chromium dioxide, CrO_2, supported on titania was prepared by impregnation of the carrier with chromium(III) nitrate (10 wt% Cr_2O_3 on TiO_2) followed by its thermal decomposition and calcination under oxygen at 573 K. X-ray amorphous CrO_2 (ca. 95%) was found to be present after calcination. The chemical and structural changes of the supported CrO_2 phase during thermal treatment in hydrogen, oxygen, air, argon, and ammonia, and under SCR conditions (selective catalytic reduction of NO by NH_3 in excess oxygen) were investigated by thermoanalytical methods, (ferro)magnetic resonance, XRD, and UV–visible and IR spectroscopy. Supported CrO_2 is reversibly reduced under hydrogen, producing antiferromagnetic CrOOH on titania. Reoxidation to CrO_2 occurs at temperatures above 520 K in air, under oxygen, and under SCR conditions (NO + NH_3 + O_2). CrOOH and CrO_2 were decomposed at $T \approx 770$ K under argon to antiferromagnetic Cr_2O_3; the decomposition is complete only at $T > 1000$ K. The composition and thermal stability of the supported oxides are compared to the corresponding bulk phases CrO_x.

INTRODUCTION

The characterization of chromium oxides supported on metal oxide surfaces is extensively reported in the literature, largely due to their activity in several catalytic processes. Although the structure of the supported phases was investigated in detail, the nature of the supported chromium oxide species remained debatable in many cases. Supported chromium species are typical of a pronounced oxidation–reduction chemistry. When chromium is supported on Al_2O_3, SiO_2, ZrO_2, or TiO_2, more than a single oxidation state is observed in most cases, depending on Cr loading, preparation procedure, and treatment conditions applied (see, e.g., Refs. (1–12) and literature cited therein). In general, Cr(III) and Cr(VI) and the corresponding oxidic phases Cr_2O_3 and CrO_3 and chromates(VI) were regarded as the main components, but also Cr(V) and Cr(II) surface species were proven or proposed to be present in nonnegligible amounts.

Chromium(IV) dioxide, CrO_2, supported on a metal oxide surface is not discussed in the literature apart from two exceptions: (i) minor amounts of CrO_2 were observed as an intermediate of CrO_3 decomposition on SiO_2 by XRD (5); (ii) in Parts I and II of this series, the presence of ferromagnetic CrO_2 was proposed hypothetically for higher-loaded oxygen-calcined CrO_x/TiO_2 catalysts for the selective reduction of NO by ammonia based on paramagnetic resonance (12) and thermoanalytical investigations (13). Very recent investigations of the products of thermal decomposition and calcination of bulk chromium(III) nitrate under conditions generally used for the preparation of supported catalysts showed Cr_2O_3 and CrO_2 to be the main products (14, 15). In addition, the specific reversible interconversion $CrO_2 \rightleftharpoons$ CrOOH could be proven also for the amorphous oxide phases, which is of special importance for the investigation of corresponding supported systems.

The hypothetical character of the supported CrO_2 surface species and the recent results of chromium(III) nitrate decomposition prompted us to investigate in detail the nature and the related interconversions of the relevant chromium oxide phases on titania using thermogravimetry (TG) and differential thermal analysis (DTA) monitored by mass spectrometry (MS), X-ray powder diffraction (XRD), (ferro)magnetic resonance, and UV–visible and FT-IR spectroscopy. Considering the distinctive magnetic properties of the three oxides concerned (CrO_2, CrOOH, and Cr_2O_3) and the high sensitivity of the method, magnetic resonance experiments are a suitable tool for characterization, especially of the supported oxides. CrO_2 is ferromagnetic below its Curie temperature $T_C \cong 390$ K (16), a property never established for any other chromium oxide.

[1] Present address: Fritz Haber Institute, Max Planck Society, Faradayweg 4-6, D-14195 Berlin, Germany.

[2] To whom correspondence should be addressed.

0021-9517/95 $12.00

CrOOH and Cr_2O_3 are typical antiferromagnetic materials with Néel points $T_N \cong 130$ (17) and 308 K (18), respectively.

Of central interest were the solid state reactions, such as the reversible interconversion $CrO_2 \rightleftharpoons$ CrOOH and the thermal decomposition of both into Cr_2O_3. The application of the results gathered for the bulk solids (15) should provide, at least for higher Cr loadings (5–10 wt%), the conditions necessary to prepare supported chromium oxide catalysts containing the desired chromium oxide phases CrO_2, CrOOH, and Cr_2O_3, as well as mixtures of defined composition on titania. In addition, the nature of the supported oxide phases has been investigated under conditions typical of the selective catalytic reduction (SCR) of nitric oxide by ammonia in excess oxygen, i.e., their transformations under ammonia and $NH_3/NO/O_2$ atmospheres.

METHODS

The starting material was prepared according to Ref. (12) by impregnation of TiO_2 (P25, specific surface area 49 m^2/g, supplier Degussa) with chromium(III) nitrate, $Cr(NO_3)_3 \cdot 9H_2O$ (Fluka). After vigorous stirring for 2 h the water was evaporated at 50 Torr (6.66×10^3 Pa) by heating to 363 K within ca. 4 h. Crushing and sieving to 0.3- to 0.5-mm grain size was followed by rapid heating to 573 K in a nitrogen stream (50 ml/min). Afterward the sample was cooled to room temperature and calcined in an oxygen stream (50 ml/min) at 573 K for 3 h (sample designation: CrO_2-ST). A chromium content of 6.84 wt% Cr = 1.46×10^{-3} mol Cr/g TiO_2 (corresponding to 10 wt% of Cr_2O_3) was used.

Thermal analytical investigations were carried out in hydrogen, air, argon, and ammonia (0.09 vol% in argon), and under a SCR atmosphere (900 ppm NO, 900 ppm NH_3, 1.8 vol% O_2, balance argon) at different temperatures and under different conditions (see later text).

The decomposition of the supported chromium oxides was investigated under pure argon (less than 0.005 vol% of impurities) and their reactions with pure hydrogen (<0.005 vol% of impurities) were carried out on a thermobalance or in a specially constructed quartz microreactor.

Preparation conditions and compositions of the different samples prepared (all of them containing an amount of Cr equivalent to 10 wt% Cr_2O_3) are summarized in Table 1. The acronyms used to designate the individual CrO_x/TiO_2 samples were derived from the main component (CrO_2-ST, CrOOH-ST, CrO_2-RE; ST means standard, RE reoxidized, and HT after high-temperature reduction) or from the percentage of these oxides remaining after decomposition under argon (error, $<\pm 5\%$).

The unsupported (bulk) oxides CrO_2 and CrOOH were prepared as follows: CrO_2 (Aithaca Chemical Corp., USA) was heated in air at 673 K prior to further use, in order to decompose the CrOOH present and to remove the organic impurities. CrOOH was prepared by reduction of CrO_2 with pure hydrogen by heating at a rate of 10 K/min in the range 298–623 K. XRD analysis confirmed the presence of only one phase in both samples (compare also Ref. (15)).

Thermoanalytical measurements were performed at a heating rate of 10 K/min on either a Mettler 2000C thermoanalyzer or a Netzsch STA 409, using α-alumina as a reference. Evolving gases were monitored on-line using a Balzers QMG 420 quadrupole mass spectrometer connected to the thermoanalyzer by a heated capillary.

X-ray analysis was carried out on a Siemens D5000 powder X-ray diffractometer using Cu$K\alpha$ radiation in step mode between 20° and 80° 2θ, with a step size of 0.01° and a step time of 0.3 s.

The content of CrO_2 and CrOOH in the samples was determined by temperature-programmed decomposition monitored by mass spectrometric (Balzers GAM 455) analysis of the evolved O_2 and H_2O. The catalyst was heated in a fused quartz microreactor at a heating rate of 10 K/min under flowing helium (300 ml/min STP).

Ferromagnetic and paramagnetic resonance spectra were recorded on Bruker ESP300 and ESP300E systems at X-band frequency (Varian E-9 spectrometer at Q-band frequency) at temperatures between 130 and 420 (300) K with microwave frequency about 9.4 (35.5) GHz, microwave power $\leq$ 1 mW, and modulation frequency 100 kHz, where the numbers in parentheses refer to Q-band measurements. The measurements were carried out in a Bruker TE104 double rectangular cavity and a modified Varian E-266 Q-band TE011 (right circular cylinder) cavity, respectively. The g values were determined with a NMR magnetometer and DPPH as a g marker. The signal intensity was obtained by numerical double integration of the sample and reference (DPPH) spectra, using the ESP300 software.

The UV–visible spectra were recorded on a spectrometer equipped with an integration sphere (Perkin–Elmer, Model Lambda 16). The diffuse reflectance spectra were recorded under ambient conditions using $BaSO_4$ as a reference. For simulation and presentation the spectra were transformed to the Kubelka–Munk function. The composite profile was fitted by a superposition of Gaussian bands (19), with the frequency positions, intensities, and linewidths being varied by the fit. A minimum number of bands were allowed to achieve adequate representation of the spectra.

The infrared spectra (transmission mode) were taken under ambient conditions using self-supporting 13-mm pellets as well as 0.5 wt% KBr pellets on Perkin–Elmer FTIR 2000 equipment. Fewer than 10 scans were collected for each spectrum at a resolution of 4 cm^{-1}.

TABLE 1

Composition of Titania-Supported CrO_x Samples

Label[a]	Preparation conditions	Composition (at.% Cr)[b]
CrO_2-ST	Impregnated sample calcined under O_2, 573 K, 3h	CrO_2: 95%, chromates(VI): 4%
CrOOH-ST	CrO_2-ST, H_2, 523 K, 1 h	CrOOH: 88%, CrO_2: 12%
CrO_2-RE	CrOOH-ST, air, 520 K, 1 h	CrO_2: 94%, CrOOH: 6%
CrO_2-27	CrO_2-ST, Ar, 773 K, 1 h	Cr_2O_3: 73%, CrO_2: 27%
CrO_2-22	CrO_2-ST, Ar, 773 K, 5 h	Cr_2O_3: 78%, CrO_2: 22%
CrOOH-24	CrOOH-ST, Ar, 773 K, 1 h	Cr_2O_3: 73%, CrOOH: 24%, CrO_2: 3%
CrOOH-15	CrOOH-ST, Ar, 773 K, 5 h	Cr_2O_3: 83%, CrOOH: 15%, CrO_2: 2%
CrOOH-HT	CrO_2-ST, H_2, 773 K, 0.25 h, Ar, 773 K, 5 h	Cr_2O_3: 79%, CrOOH: 19%, CrO_2: 2%

[a] The acronyms used to designate the individual CrO_x/TiO_2 samples were derived from the main component CrO_2 or CrOOH. ST indicates the standard sample containing the maximum amount of the main component; the numbers, e.g., 27 or 22, express the atomic percentage of the oxide remaining after decomposition of the ST samples. RE means after reoxidation of CrOOH-ST, and HT means after high-temperature reduction of CrO_2-ST.

[b] Quantitative composition derived from thermal analysis monitored by mass spectrometry.

RESULTS

Thermal Analysis of the Supported Chromium Oxide Phases

After calcination under oxygen. All these investigations started from a sample prepared by the impregnation of TiO_2 with $Cr(NO_3)_3 \cdot 9H_2O$ (Cr content ca. 7 wt% Cr/TiO_2, i.e., 10 wt% Cr_2O_3/TiO_2) followed by drying and calcination under oxygen at 573 K, as described under Experimental and in further detail in Ref. (12). The thermogravimetric curve (TG) of the sample shows that the loss of weight occurs in two stages (Fig. 1). During the first stage, physisorbed water evolves from the support (mass spectrometric curve, m/z = 18) with a peak centered at T = 406 K. The amount of desorbed water is estimated to be 0.8–0.9 wt%. The second step starting at 553 K is caused by the evolution of oxygen (m/z = 32), which is interpreted in accordance with the magnetic and spectroscopic results as being due to CrO_2 decomposition (see below). The maximum rate of oxygen evolution occurs at 680 K, a temperature significantly lower than that found for bulk, crystalline CrO_2 (ca. 770 K), but comparable to that observed for amorphous CrO_2 (15). The completion of the CrO_2 decomposition at about 1070 K indicates a significant stability of CrO_2 supported on titania. Although XRD analysis of the sample designated as CrO_2-ST did not show any patterns different from those of the carrier (anatase and rutile) indicating the poor crystallinity (X-ray amorphous nature) of the supported chromium oxide, additional patterns arising from crystalline Cr_2O_3 appeared after heating to 1170 K (inset of Fig. 1B). The mass spectrometric curve m/z = 44 indicates desorption of CO_2, the amount of desorbed CO_2 corresponding to only 1/20 of the oxygen evolution.

Mass spectrometric detection of the evolved gases showed that the amount of oxygen released corresponded to 1.01 wt% referred to total weight or 10.55 wt% referred to CrO_2. This result indicates that 95% of the chromium was present as CrO_2 before decomposition. The oxygen evolution occurred in two discernible steps in the range

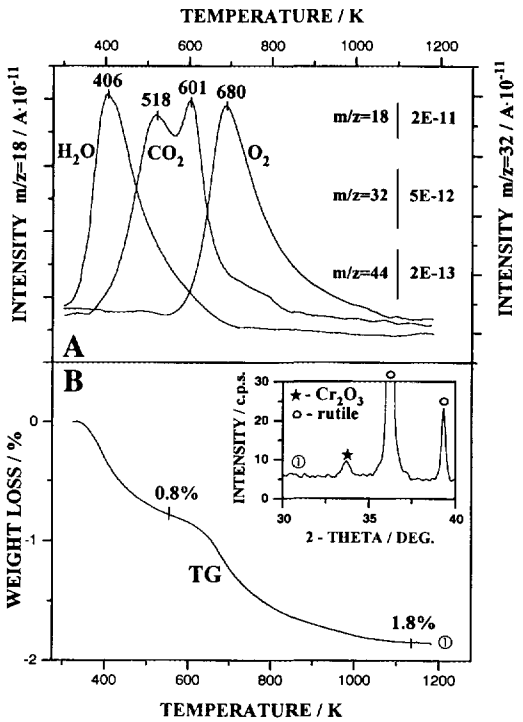

FIG. 1. Decomposition of CrO_2-ST under argon. (A) Mass spectrometric (m/z = 18, 32, and 44) and (B) thermoanalytical measurements. The cutout of XRD patterns of the product after heating to 1170 K shown as an inset (upper right of (B)) indicates the presence of Cr_2O_3. The notation 2E-11, 5E-12, etc. signifies 2×10^{-11}, 5×10^{-12}, etc.

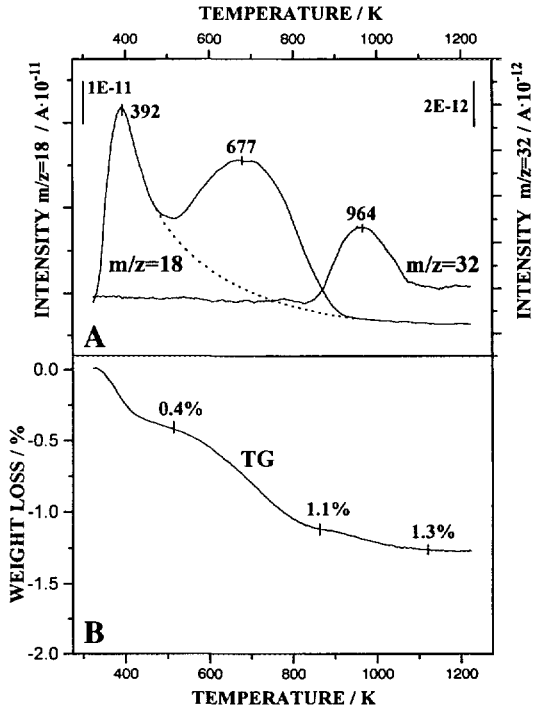

FIG. 2. Decomposition of CrOOH-ST under argon. (A) Mass spectrometric (m/z = 18 and 32) and (B) thermoanalytical results.

513–1093 K. The decreasing rate of CrO_2 decomposition with increasing conversion was described and explained in the literature for bulk crystalline (20) and amorphous chromium dioxide (15). With preceding decomposition the crystallographic shear planes formed in the CrO_2 rutile-type structure close the empty tunnels running parallel to the c-axis and suppress the rate of oxygen evolution. As a consequence, the decomposition of the last 10–15% of the chromium dioxide requires temperatures higher than 870 K for a non-isothermal run. Even under long-term isothermal conditions it is therefore rather impossible to decompose the supported CrO_2 completely without increasing the temperature above 770 K.

After reduction under hydrogen (redox cycle $CrO_2 \rightleftharpoons$ CrOOH). The mutual interconversion of CrO_2 and CrOOH has been shown to be very characteristic and suitable for the identification of both chromium oxide phases (15, 20, 21). Therefore, the CrO_2 on the calcined sample (CrO_2-ST) was reduced to CrOOH under pure hydrogen at 523 K for 1 h (see Table 1). Higher temperatures enhance the decomposition of the product CrOOH. The TG curves of the resulting sample CrOOH-ST (Fig. 2) indicate three distinct stages of weight loss: (i) the desorption of physisorbed water (m/z = 18) from the support (0.4 wt%, shown by the dashed line in Fig. 2), (ii) the evolution of water mainly formed by the decomposition of CrOOH between 470 and 940 K (0.7 wt%), and (iii) the evolution of oxygen between 820 and 1090 K (0.2 wt%).

The sample was reoxidized in air at 520 K for 1 h. The thermoanalytical curves of the reoxidized sample (Fig. 3) indicate the presence of residual CrOOH after oxidation (small peak centered at 615 K, m/z = 18, above the dashed line continuing the desorption peak of physisorbed water). The curve m/z = 32 indicates the decomposition of CrO_2. The maximum of the corresponding oxygen evolution occurs at 700 K. From the mass spectrometric data it can be calculated that two chromium-containing phases, CrO_2 (94%) and CrOOH (6%), were present after reoxidation of CrOOH/TiO_2 (CrO_2-RE).

Preparation of Chosen (Mixed) Chromium Oxide Phases Supported on Titania

Starting from the results presented above concerning the reactions of CrO_2 and CrOOH supported on titania, two series of catalysts containing the chromium oxide phases CrO_2, CrOOH, and Cr_2O_3 with defined composition were prepared. First, the sample calcined under oxygen containing mainly CrO_2 (about 95%, CrO_2-ST) was decomposed under argon at 773 K for 1 and 5 h, respectively. Second, the calcined sample subsequently reduced under hydrogen and containing mainly CrOOH was decomposed under argon as well as reoxidized in air. The

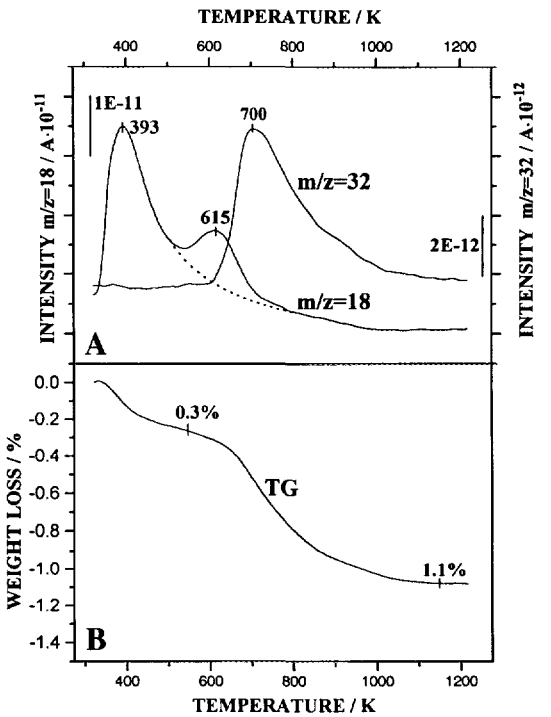

FIG. 3. Decomposition of CrO_2-RE (CrOOH-ST after reoxidation in air). (A) Mass spectrometric (m/z = 18 and 32) and (B) thermoanalytical results.

conditions applied and the composition of the prepared catalysts as deduced from the thermoanalytical and mass spectrometric measurements are summarized in Table 1. Concerning the choice of the conditions the following features had to be taken into account. All conversions had to be performed under conditions as mild as possible in order to avoid undesired changes in the supported system (see above). The preparation of CrOOH via the reaction of CrO_2 with hydrogen had to be performed at temperatures below 525 K because CrOOH starts to decompose already at this temperature under hydrogen (15), and even at 470 K under Ar. This does not allow the completion of the reduction. Note that the above-mentioned specific features of the decomposition of CrO_2 restrict the maximum yield. Temperature and duration used for the thermal decomposition of supported CrO_2 and CrOOH are further restricted if agglomeration and crystallization of the product Cr_2O_3 must be avoided. Despite these limitations the solid state reactions used afforded high yields even under mild conditions. Catalysts containing the desired phase, i.e., CrO_2, CrOOH, or Cr_2O_3, in concentrations higher than 80–90% could be prepared (Table 1).

Beha ior of the Chromium Oxide Phases in Ammonia and SCR Atmosphere

In order to examine the possibility of the reduction of CrO_2 by ammonia and the oxidation of CrOOH under SCR conditions, the respective reactions were studied with the corresponding unsupported (bulk) materials. The assumption that the reactivities of bulk and surface phases are similar seems to be justified considering the qualitative agreement between the reactivities of the unsupported and supported samples described above (compare also Ref. (15)). The products of the corresponding experiments with the supported chromium oxide phases were investigated

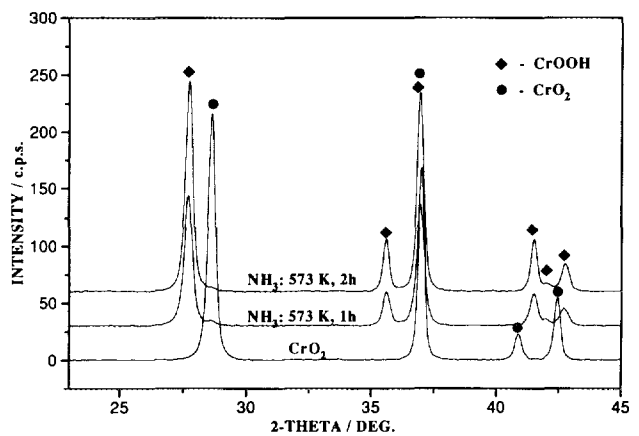

FIG. 4. XRD patterns of unsupported CrO_2 before and after exposure to ammonia (0.09 vol% under Ar) at 573 K for 1 and 2 hours, respectively.

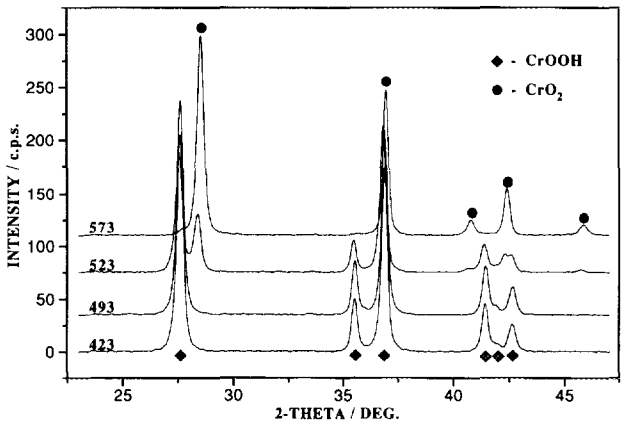

FIG. 5. XRD patterns of unsupported β-CrOOH after exposure to SCR feed gas (0.5 vol% NH_3, 0.09 vol% NO, 1.8 vol% O_2, balance Ar) at different temperatures for 1 hour.

by magnetic resonance (see below), which confirmed this assumption. For the reduction of CrO_2, ammonia with a concentration of 0.09 vol% (balance Ar) was used instead of hydrogen. Ammonia was passed with a flow rate of 50 ml/min at 573 K through a bed of 100 mg of CrO_2 placed in the microreactor. XRD patterns of the samples, taken after 1 and 2 h, are shown in Fig. 4. Even under these mild conditions (low ammonia concentration), chromium dioxide is almost completely converted to CrOOH after 1 h. After 2 h on stream the sample showed only the most intense CrO_2 reflection (2θ = 28.64) besides β-CrOOH.

The ease of the CrOOH oxidation prompted us to investigate its reactivity in typical SCR feed gas (0.05 vol% NH_3, 0.09 vol% NO, 1.8 vol% O_2, balance Ar). XRD patterns of the sample after heating it under an SCR atmosphere (flow 100 ml/min STP, duration 1 h) at various temperatures are displayed in Fig. 5. Even in the presence of the reducing agent (ammonia) and despite the low oxygen concentration, chromium dioxide, the product of CrOOH oxidation, is detected at 523 K. For the sample exposed at 573 K only a residual amount of CrOOH is observed.

Magnetic Resonance

Calcined sample. The ferromagnetic resonance (FMR) powder spectra of the calcined sample at the frequency ν = 9.4 GHz are shown in Fig. 6A for different recording temperatures and at ν = 35 GHz in Fig. 6 B for T = 293 K. As expected for a ferromagnetic (or superparamagnetic) system and analogously to other FMR investigations of CrO_2 (23–27), they are strongly temperature dependent concerning the width, shape, and intensity (numerical double integral) of the lines. Above 390 K, the Curie temperature (T_C) of CrO_2, a symmetric derivative line is observed: T = 400 K; g = 1.972, and ΔB_{pp} = 23 mT. Below 390 K

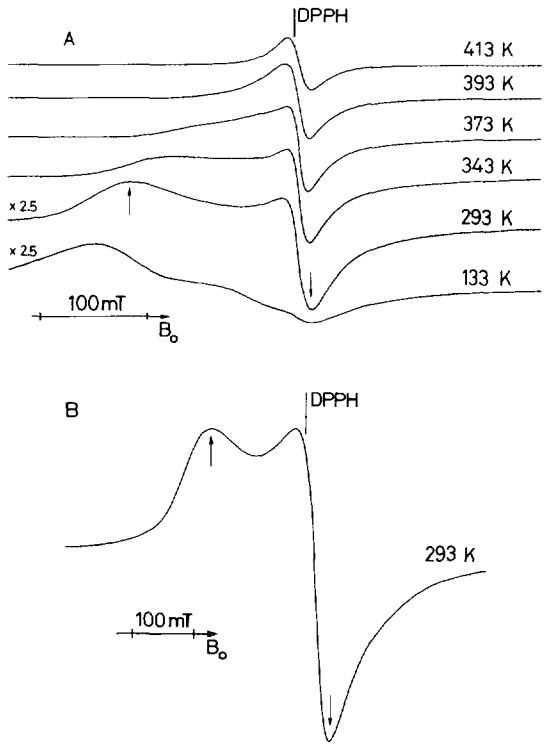

FIG. 6. Ferromagnetic resonance spectra of the impregnated sample calcined under oxygen at 573 K (CrO_2/TiO_2, CrO_2-ST) for different recording temperatures (A) at X-band (ν = 9.4 GHz) and (B) at Q-band (ν = 35.6 GHz). The arrows indicate where the ΔB_{pp} values were taken from.

the line is broadened, becomes first asymmetric and for T < 353 K a low-field shoulder appears and is further shifted to lower fields against the derivative line remaining at g = 1.98 (ΔB_{pp} = 30 mT) with decreasing temperatures. A finite value of absorption is observed at zero field at the lowest temperature investigated in the X band (T = 133 K). The temperature dependence of ΔB_{pp} is given in Fig. 7. This peak-to-peak linewidth, ΔB_{pp} or H_{an}, which is ordinarily deduced from the ferromagnetic resonance powder spectra as indicated by arrows in Figs. 6A and 6B (22), is caused by a number of different magnetic anisotropies. Their main contributions to ΔB_{pp} are not markedly field dependent to a first approximation, as can be seen from the FMR spectra at a frequency of 35.5 GHz (Fig. 6B). The low-field shoulder appears at B = 1.08 T and the corresponding derivative line at 1.26 T (g = 1.975), i.e., the ΔB_{pp} value defined above is practically unchanged for both frequencies used. Additionally this proves that this low-field absorption is not due to a new or different signal or compound.

The temperature dependence of the integrated intensity at ν = 9.4 GHz is shown in Fig. 7 as $I_{rel} = I(T)/I(T_0)$ versus T (T_0 = 130 K, lowest T investigated). The determination of the Curie temperature T_C of the supported CrO_2, using as a first approximation a linear extrapolation of the linewidth $\Delta B_{pp} \propto T$ (25), yields a $T_C \cong 400$ K, which is slightly higher than that of pure bulk CrO_2 (16). A direct proportionality of ΔB_{pp} holds, however, only in the case of pure shape anisotropy. For CrO_2 embedded in a polymer matrix (25), however, it has been found that all anisotropies, i.e., shape, magnetocrystalline, and magnetostriction, must be taken into account. The field H_{an} (ΔB_{pp}) > 200 mT is also too large to be explained by magnetocrystalline anisotropy alone (27). The determination of T_C by the quadratic (22) or cubic (28, 29) extrapolation of I_{rel} yields T_C values lower than that of bulk CrO_2 ($T_C \approx 360$ K or lower). At this point it must be mentioned that the magnetic characteristics such as $\Delta B_{pp} \propto T$ and $I_{rel} \propto T$ depend sensitively on slight, more or less controllable changes of the preparation conditions (impregnation, drying, calcination). This is found as a result of several repetitions of the preparation procedure. The particle size of CrO_2 calculated from the I_{rel} versus T dependence using the Langevin function $L(X)$ (22, 30) assuming superparamagnetism and single-domain particles, varies accordingly (particle diameter of a few nanometers). On the other hand, repeated calcination under oxygen caused similar magnetic parameters for all samples prepared (T_C increases).

More quantitative statements concerning the kind of anisotropy, particle size and distribution, and crystallization effects and their dependence on chromium content and pretreatment require more detailed investigation and interpretation and will be discussed elsewhere. At this point the following needs to be stated. The observed resonance spectra are clearly due to collective properties of a ferromagnetic system. Chromium dioxide is the only known transition metal oxide that is strongly ferromagnetic at room temperature. There is no indication of the presence

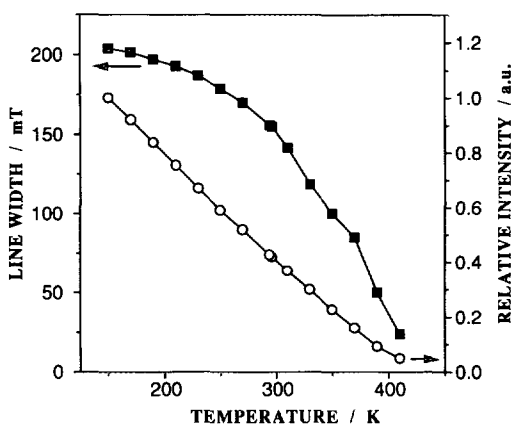

FIG. 7. Temperature dependence of the integrated intensity of the FMR spectra (thermomagnetic curves, empty circles) and of the linewidths (ΔB_{pp}, peak to peak, full squares) for a typical CrO_2/TiO_2 sample.

of other magnetic components, such as Cr(III) or Cr_2O_3, as found for the corresponding calcination product of bulk chromium nitrate. As a restriction it must be mentioned, however, that diamagnetic components such as chromates(VI) would not be observable by EPR/FMR, and that minor amounts of paramagnetic or antiferromagnetic constituents could be masked by the strong ferromagnetic absorption.

Magnetic resonance of the intercon ersion products. The spectra after the reduction of the calcined sample under hydrogen at T = 523 K for 1 h (CrOOH-ST) are shown in Fig. 8 for different recording temperatures. The spectra are symmetric Lorentzian lines whose width and intensity are temperature dependent. The peak-to-peak linewidth increases with decreasing temperature from about 70 mT at 293 K to 90 mT at 130 K (spectrum not shown) but remains symmetric over the full temperature range investigated. This indicates that Cr^{3+} ions coupled antiferromagnetically by exchange interactions. The signals are assigned to Cr^{3+}–O^{2-} clusters (β phase (1)). The behavior observed is expected for minute β-CrOOH particles, which do not exhibit distinct magnetic properties, such as a sharp Néel point. There is no indication of a chromium oxidation state other than +3 by EPR or by any other spectroscopic method applied. Very low amounts of CrO_2, however, would not be expected to be observable under the conditions applied. The same spectroscopic features were observed for CrO_2-ST after reduction with ammonia (T = 573 K, 2 h).

The spectra of the reduced sample (CrOOH-ST) decomposed under argon under mild conditions depend on the temperature and duration of the treatment. Three samples will be compared (Fig. 9): decomposition of CrOOH-ST (i) for 1 h at T = 773 K under Ar (CrOOH-24), (ii) for 3 h at T = 773 K under Ar (CrOOH-15), and (iii) a sample prepared by reduction of CrO_2-ST at a temperature as high as 773 K (CrOOH-HT). The temperature dependence of the linewidths ΔB_{pp} (Fig. 9A) and integrated intensities (Fig. 9B) become gradually more similar to antiferromagnetic Cr_2O_3 from (i) to (iii) (compare, e.g., solid solutions of Cr_2O_3 in Al_2O_3 (31, 32)). The quantitative interpretation of the antiferromagnetic resonance data of α-Cr_2O_3 is reported for rather large grain sizes (a few tenths to a few hundreds of nanometers in diameter (33)) of crystalline samples. The sizes of the supported CrOOH and Cr_2O_3 clusters described above are expected to be a few nanometers only (from FMR measurements of the CrO_2 precursor CrO_2-ST and from the temperature dependence of the FMR spectra). This does not allow quantitative statements. However, the qualitative information obtained is unambiguous: in all samples described we can observe a more or less pronounced antiferromagnetic behavior typical of chromium(III)–oxygen clusters of different sizes. The decomposition at high temperatures (1170 K) causes a magnetic behavior typical of crystalline α-Cr_2O_3 (18) (data not shown), which is in agreement with the corresponding XRD (inset Fig. 1B), and the reduction of CrO_2-ST at $T \geq$ 773 K causes a pronounced antiferromagnetic behavior, indicating an increase in the particle size of Cr_2O_3 on the surface.

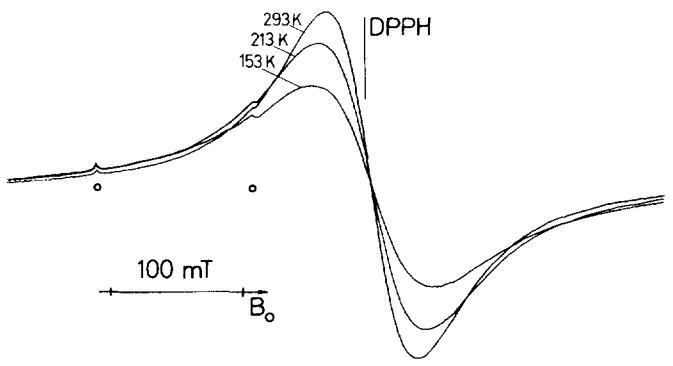

FIG. 8. Paramagnetic resonance spectra of CrOOH-ST for different recording temperatures at X-band (ν = 9.4 GHz). The small peaks indicated by open circles are due to Cr^{3+} incorporated into the lattice of rutile (compare with (12) and literature cited therein).

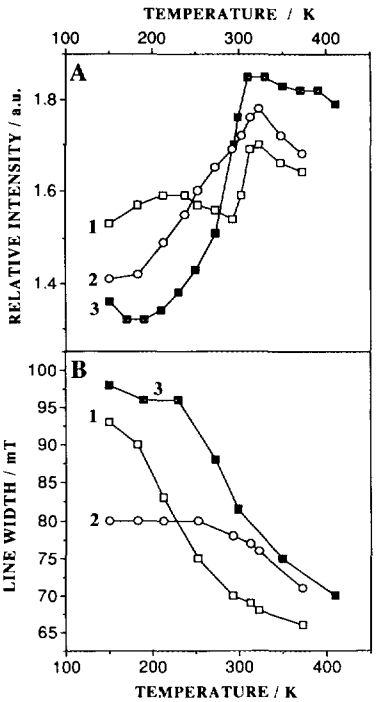

FIG. 9. Temperature dependence (A) of the integrated intensity of the magnetic resonance spectra and (B) of the linewidths (ΔB_{pp}) for the decomposition of CrOOH-ST (1) for 1 h at T = 773 K in Ar (CrOOH-24), (2) for 5 h at T = 773 K in Ar (CrOOH-15), and (3) for the sample prepared by reduction of CrO_2-ST at T = 773 K in hydrogen followed by decomposition under Ar for 5 h at 773 K (CrOOH-HT).

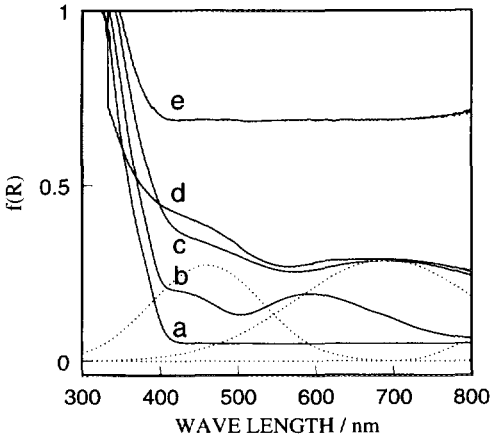

FIG. 10. UV–visible diffuse reflectance spectra of (a) pure titania support (calcined), (b) impregnated sample, (c) CrOOH-ST, (d) products of decomposition of CrOOH under argon (CrOOH-24), (e) CrO_2-ST. For spectrum (c) two bands resulting from the deconvolution analysis are given (dashed lines). The fit procedures were performed after subtracting the TiO_2 background.

Reoxidation and SCR conditions. Reoxidation of CrOOH-ST in air or under oxygen gives samples having practically the same spectroscopic features of ferromagnetic CrO_2 as described for the oxygen-calcined sample. The same is true for the sample exposed to an SCR atmosphere containing 900 ppm NO, 900 ppm NH_3, and 1.8 vol% oxygen under argon for temperatures above 573 K (1 h). For $T < 473$ K, the magnetic properties typical of a antiferromagnetic material (CrOOH, compare above) are observed; for temperatures between 473 and 573 K, the CrOOH species were oxidized under SCR conditions to ferromagnetic CrO_2. That means that as regards the nature and oxidation state of the chromium surface species the SCR atmosphere is oxidative in character above temperatures of about 523 K even in the presence of the reducing agent NH_3.

UV–Visible Spectroscopy

The observed changes in color of the samples are in all cases in agreement with the results reported above. After calcination (CrO_2-ST) the sample is black as bulk CrO_2. The UV–visible spectrum consists of one strong, very broad absorption over the full visible range (Fig. 10e). This is attributed in the literature to highly conducting phases (5). The strong absorption does not allow the identification of charge transfer bands due to Cr(VI) components. Below 400 nm all diffuse reflectance spectra are dominated by strong absorptions of the titania carrier (Fig. 10a). Reduction under hydrogen (Fig. 10c) changes the color to green and the UV–visible absorptions with maxima at 470 and 690 nm are ascribed to the $A_{2g} \rightarrow T_{1g}$ and $A_{2g} \rightarrow T_{2g}$ d–d transitions due to Cr^{3+} (34). Particularly the latter is shifted toward higher wavelengths in comparison to bulk Cr_2O_3 or mononuclear or dinuclear Cr^{3+} in octahedral coordination in solution (about 460 and 600 nm). Thermal decomposition of CrOOH generates spectra with slightly changed band positions in comparison to CrOOH-ST (Figs. 10c and 10d; 460 and 660 nm). The assignment to Cr^{3+} is in agreement with the results described above. The shifts of the bands were observed also for other supported Cr(III)-oxide phases (34, 35) and will not be further discussed here.

FT-IR Spectroscopy

The most pronounced absorptions in the transmission IR spectra of self-supporting and KBr pellets expected for CrOOH, Cr_2O_3, or CrO_2 are covered by the strong titania absorptions below 800 cm^{-1}, between 3500 and 2900 cm^{-1} and around 1600 cm^{-1} (OH and H_2O vibrations). One pronounced band (also observed in pure CrO_2 KBr pellets) is always observed, however, in the oxygen-calcined sample at 943 cm^{-1}. It disappears reversibly upon reduction under H_2 and also by decomposition under argon at higher temperature. It is interpreted as an IR indication of CrO_2 in the calcined sample.

Cr(VI) Surface Species

Although no evidence for Cr(VI) could be found from UV–visible diffuse reflectance spectra (strong absorption and bad reflectivity of black CrO_2), there is indication that after calcination a nonnegligible amount of chromium(VI) is present in the calcined sample (CrO_2-ST). This is indicated by the immediate dissolution of only slightly bound Cr(VI) species from the surface in aqueous suspensions of this catalyst as already described in the literature (5, 12). The Cr(VI) content of about 4 wt% of total chromium derived from UV–visible spectroscopic and AAS measurements of the supernatant solution after centrifugation (standard calibration curves) is in good agreement with the quantitative determination of CrO_2 by thermoanalytical and mass spectrometric methods (95 wt% CrO_2). CrO_2 should not be influenced by this procedure; it is transformed to CrOOH only after days in hot water (16).

DISCUSSION

The thermal decomposition of chromium(III) nitrate, which is a widely used precursor for supported chromium oxide catalysts, is known to occur via complex denitration and dehydration processes (15), and literature cited therein). For chromia deposited on an oxidic support using comparatively high temperatures and chromium contents, mainly chromates(VI) and Cr_2O_3 were reported in the literature. In the present paper it has been shown unambiguously that the thermal decomposition (T = 573 K) of chromium(III) nitrate impregnated onto titania with ca. 7

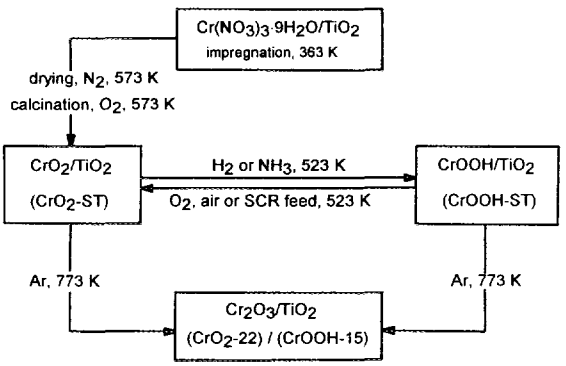

SCHEME 1. Interconversions of titania supported chromium oxide phases occurring under specified conditions.

wt% Cr loading followed by calcination under oxygen at 573 K leads to the information of mainly CrO_2 (95%; minor amounts of chromium(VI) only).

The presence of the X-ray amorphous CrO_2 on TiO_2 has been experimentally proven by several methods. Chromium dioxide, CrO_2, is the only known transition metal oxide which is strongly ferromagnetic at room temperature. There is no doubt that the ferromagnetic behavior of the CrO_x/TiO_2 sample observed by magnetic resonance (Figs. 6 and 7) is due to CrO_2. The poor crystallinity of the supported chromium dioxide phase is confirmed by XRD and by particle sizes of a few nm diameter estimated from the thermomagnetic curves (Fig. 7). Characteristic features of CrO_2 were also obtained from UV–visible diffuse reflectance (black color) and FT-IR spectroscopy. Further confirmation of the presence of CrO_2 on titania is obtained from thermoanalytical measurements (oxygen evolution during thermal decomposition, Figs. 1 and 2) as well as from the specific reversible interconversion $CrO_2 \rightleftharpoons$ CrOOH. The former allowed the quantitative determination of the CrO_2 content, and the latter indicated the way to prepare defined supported CrOOH on titania.

The chemical reactions performed starting from the CrO_2/TiO_2 system (CrO_2-ST) are summarized in Scheme 1. By analogy with bulk chromium dioxide, CrO_2 supported on titania is reducible to CrOOH under hydrogen at $T = 523$ K. The facile interconversion of the tetragonal chromium dioxide to an orthorhombic CrOOH is explained on the basis of the close similarity of their structures (20, 21). The problem of the thermal stability of both compounds (irreversible decomposition to Cr_2O_3) restricts the temperature that can be applied, but under carefully chosen experimental conditions yields of ca. 90% (Fig. 2, Table 1) could be achieved as in the case of the unsupported phase. XRD data (not presented) and magnetic measurements (Fig. 9) indicate that under hydrogen ($T = 773$ K) the crystallite size of Cr_2O_3 increases. The reduction can be performed even with 0.09 vol% NH_3 under argon at 573 K. Practically complete reoxidation to CrO_2 is possible at temperatures above 523 K under oxygen, in air (Fig. 3), and even under SCR conditions, i.e., in the presence of the reducing ammonia and in spite of the low oxygen concentration. The reduction of CrO_2 by NH_3 and the oxidation of CrOOH under SCR conditions is clearly proven by XRD for the bulk CrO_2 and CrOOH (Figs. 4 and 5) and by the magnetic and spectroscopic features for the supported oxide phases. Due to the specific magnetic properties of the chromium oxides considered, i.e., the antiferromagnetism of Cr_2O_3 and CrOOH and the ferromagnetism of CrO_2, and due also to the high sensitivity of the technique, magnetic resonance is found to be a very suitable method for the identification of the supported crystalline and amorphous chromium oxide phases.

Again in accordance with the bulk oxides, supported CrOOH and CrO_2 decompose under an inert atmosphere into Cr_2O_3 in a wide temperature range. The courses of the thermoanalytical curves presented in Figs. 1 and 2 indicate that temperatures higher than 1000 K are necessary for total conversion of CrO_2. This is important for the selective preparation of supported chromium oxide phases starting from CrO_2, because temperatures that are too high can cause undesired changes in the surface area, porosity, and microstructure of the catalyst as well as of the particle size of the supported chromium oxide. On the other hand, the presence of a CrO_2-like phase must be taken into account even after a treatment at rather high temperatures once CrO_2 had been formed during the catalyst preparation procedure. The formation of Cr_2O_3 from CrO_2 is irreversible and is not complete under mild conditions ($T < 770$ K) even after several hours. Much higher temperatures are required to complete this decomposition, which in turn increases the crystallite size of Cr_2O_3 on the surface of titania (Fig. 1B, inset).

The similarity of solid state reactions for bulk and supported samples such as the interconversion $CrO_2 \rightleftharpoons$ CrOOH and the decomposition of these compounds to Cr_2O_3 showed for the first time a way to prepare rather pure CrO_2 and CrOOH phases supported on an oxide surface. It demonstrates that the synthesis method and conditions of calcination especially for moderate temperatures can be very important for the structure and composition of supported metal oxide catalysts. It is interesting to compare the reactivity of bulk (15) and supported chromium oxides at this point. It is evident that the properties and conversion conditions of the chromium oxide phases supported to ca. 7 wt% Cr on titania are practically the same as for bulk materials. All solid state reactions and decomposition processes occur in a very similar temperature range under the chosen atmospheres. Differences between the bulk and the surface systems are observed, however, when violent crystallization effects of CrO_2 combined with its rapid decomposition to Cr_2O_3 are involved. This

is manifested by different decomposition products of chromium(III) nitrate, which consist of Cr_2O_3 and CrO_2 in the bulk system, whereas only CrO_2 (besides Cr(VI)) is found on the surface of titania. Probably, the heat evolved by crystallization cannot be removed fast enough in the bulk system (much larger heat generation per volume of solid), and the resulting increase in the sample temperature increases the rate of decomposition of CrO_2. Also, the limited mobility of CrO_2, preventing rapid crystallization in the supported system, seems to play a role.

For the selective reduction of NO by ammonia over chromium oxide catalysts, the observation is important that unsupported and supported CrOOH are easily oxidized even under "reductive" conditions by small amounts of oxygen at temperatures above 523 K. This means that at least for high chromium contents at temperatures above 523 K chromium dioxide must be regarded as a possibly existing phase in addition to Cr_2O_3, which is neither oxidized by oxygen nor reduced by NH_3 or H_2 at temperatures below 1000 K.

CONCLUSIONS

Supported chromium dioxide (ca. 7 wt% of Cr) has been prepared by impregnation of titania with chromium(III) nitrate and subsequent thermal decomposition (573 K, nitrogen) followed by calcination under oxygen at 573 K. Of the supported Cr containing phases, 95% were present as CrO_2. The reduction of this phase under hydrogen and ammonia leads to CrOOH, which can be reversibly oxidized to CrO_2 under oxygen, in air, and under SCR conditions ($NO + NH_3 + O_2$). Both, CrOOH and CrO_2, supported on titania, decompose to Cr_2O_3 at higher temperatures. Under the conditions used in the thermal analytical investigations (heating rate of 10 K/min), the decomposition is complete only above ca. 1000 K. Under isothermal conditions (773 K), as generally used in catalyst preparation, ca. 20% CrO_2 remains undecomposed even after 5 h. All solid state reactions of the supported chromium oxides occur with high yields (80–90%). The reactivity of the supported and bulk oxide phases is found to be comparable for the chromium loading used. Knowledge about these solid state reactions gained from investigations of the bulk samples (15), together with a careful selection of the experimental conditions, allowed for the first time the preparation of rather pure CrO_2 and CrOOH phases supported on an oxide surface.

ACKNOWLEDGMENTS

The authors thank Professor A. von Zelewsky, University of Fribourg, and Professor R. Kirmse, University of Leipzig, for the opportunity to measure magnetic resonance spectra in their laboratories. K. K. thanks the Stiftung Stipendienfonds des Verbandes der Chemischen Industrie (Federal Republic of Germany) for a grant (Liebig-Stipendium) and Dr. W. Mörke, University of Halle-Wittenberg, for helpful discussions of the FMR spectra. Financial support of this work by the Swiss National Science Foundation is acknowledged.

REFERENCES

1. Poole, C. P., and McIver, D. S., *Ad . Catal.* **17,** 223 (1967).
2. Vuurman, M. A., Hardcastle, F. D., and Wachs, I. E., *J. Mol. Catal.* **84,** 193 (1993).
3. Grünert, W., Shpiro, E. S., Feldhaus, R., Anders, K., Antoshin, G. V., and Minachev, K. M., *J. Catal.* **100,** 138 (1986).
4. Cornet, D., and Burwell, R. L., *J. Am. Chem. Soc.* **90,** 2489 (1968).
5. Cimino, A., De Angelis, B. A., Luchetti, A., and Minelli, G., *J. Catal.* **45,** 316 (1976).
6. Zecchina, A., Garrone, E., Ghiotti, G., Morterra, C., and Borello, E., *J. Phys. Chem.* **79,** 966 (1975).
7. Cimino, A., Cordischi, D., Febraro, S., Gazzoli, D., Indovina, V., Occhiuzzi, M., Valigi, M., Boccuzzi, F., Chiorino, A., and Valigi, M., *J. Mol. Catal.* **55,** 23 (1989).
8. Cimino, A., Cordischi, D., De Rossi, S., Ferraris, G., Gazzoli, D., Indovina, V., Occhiuzzi, M., and Valigi, M., *J. Catal.* **127,** 761 (1991).
9. Hardcastle, F. D., and Wachs, I. E., *J. Mol. Catal.* **46,** 173 (1988).
10. Kim, D. S., and Wachs, I. E., *J. Catal.* **142,** 166 (1993).
11. Jagannathan, K., Srinivasan, A., and Rao, C. N. R., *J. Catal.* **69,** 418 (1981).
12. Köhler, K., Schläpfer, C. W., von Zelewsky, A., Nickl, J., Engweiler, J., and Baiker, A., *J. Catal.*, **143,** 201 (1993).
13. Engweiler, J., Nickl, J., Baiker, A., Köhler, K., Schläpfer, C. W., and von Zelewsky, A., *J. Catal.* **145,** 141 (1994).
14. Fouad, N. E., Knözinger, H., Zaki, M. I., and Mansour, S. A. A., *Z. Phys. Chem.* **171,** 96 (1991).
15. Maciejewski, M., Köhler, K., Schneider, H., and Baiker, A., *J. Solid State Chem.*, in press.
16. Chamberland, B. L., *CRC Crit. Re . Solid State Mater. Sci.* **7,** 1 (1977).
17. Christensen, A. N., *Acta Chem. Scand.* A **30,** 133 (1976).
18. Dayhoff, E. S., *Phys. Re .* **107,** 94 (1957).
19. Press, W. H., Flannery, B. P., Teukolsky, S. A., and Vetterling, W. T., "Numerical Recipes in C: The Art of Scientific Computing," p. 517. Cambridge Univ. Press, Cambridge, UK, 1990.
20. Saez-Puche, R., and Alario-Franco, M. A., *J. Solid State Chem.* **38,** 87 (1981); *J. Solid State Chem.* **47,** 59 (1983); *Thermochim. Acta* **74,** 273 (1987).
21. Tombs, N. C., Croft, W. J., Carter, J. R., and Fitzgerald, J., *Inorg. Chem.* **3,** 1791 (1964).
22. (a) Bonneviot, L., Che, M., Olivier, D., Martin, G. A., and Freund, E., *J. Phys. Chem.* **90,** 2112 (1986); (b) Bonneviot, L., and Olivier, D., *in* "Catalyst Characterization: Physical Techniques for Solid Materials" (B. Imielik and J. C. Védrine, Eds.), Chap. 7, p. 196. Plenum, New York/London, 1994.
23. Netzelmann, U., *J. Appl. Phys.* **68,** 1800 (1990).
24. Orth, Th., Netzelmann, U., Dean, B., Hoare, A., von Geisau, O., Pelzl, J., Chantrell, R. W., Veitch, R., and Jakusch, H., *J. Magn. Magn. Mater.* **101,** 235 (1991).
25. Hirschfelder, M., "Models for the Ferromagnetic Resonance of Single-Domain Particles," Thesis, Merseburg, Germany, 1990.
26. Kuznetsov, Yu. S., Viglin, N. A., Stepanov, A. P., Kitaev, G. A., and Mokhov, A. G., *Russ. J. Phys. Chem.* **50,** 1263 (1976); *Zh. Fiz. Khim.* **50,** 2109 (1976).
27. Craik, D. J., "Magnetic Oxides," Part 2, p. 729. Wiley, London, 1975.
28. Mörke, W., Vogt, F., Wendlandt, K. P., Walter, H., and Roewer, G., *J. Chem. Soc. Faraday Trans.* **89,** 1085 (1993).
29. Ibach, H., and Lüth, H., "Solid-State Physics," p. 141, Springer Verlag, Berlin, 1990.

30. Mörke, W., Hirschfelder, M., Gehre, S., and Doerffel, K., *Chemom. Intell. Lab. Syst.* **8,** 87 (1990).
31. Poole, C. P., and Itzel, J. F., *J. Chem. Phys.* **41,** 287 (1964).
32. Stone, F. S., and Vickerman, J. C., *Trans. Faraday Soc.* **67,** 316 (1971).
33. Gerling, R., and Dräger, K., *Surf. Sci.* **106,** 427 (1981).
34. Martin, C., Martin, I., Rives, V., Palmisano, L., and Schiavello, M., *J. Catal.* **134,** 434 (1992).
35. Iwasawa, Y., Sasaki, Y., and Ogasawara, S., *J. Mol. Catal.* **16,** 27 (1982).